IOP Conf. Series: Journal of Physics: Conf. Series **980** (2018) 012008 doi:10.1088/1742-6596/980/1/012008

Column formation and hysteresis in a two-fluid tornado

B R Sharifullin[1], I V Naumov[1], M A Herrada[2], V N Shtern[3]

[1]S.S. Kutateladze Institute of Thermophysics SB RAS, 630090, Russia, Novosibirsk, Lavrentyeva str., 1
[2]E.S.I, Universidad de Sevilla, Camino de los Descubrimientos s/n 41092, Spain
[3]Shtern Research and Consulting, Houston, Texas 77096, USA

E-mail: naumov@itp.nsc.ru

Abstract. This experimental and numerical study addresses a flow of water and sunflower oil. This flow is driven by the rotating lid in a sealed vertical cylinder. The experiments were performed in a glass container with a radius of 45 mm and a height of 45 mm with the water volume fraction of 20%. Different densities and immiscibility of liquids provide the stable and sharp interface. At the rest, the interface is flat and horizontal. As the rotation speeds up, a new water-flow cell emerges near the bottom center. This cell expands and occupies almost the entire water domain while the initial water circulation shrinks into a thin layer adjacent to the interface. The water, rising near the container axis, strongly deforms the interface (upward near the axis and downward near the sidewall). A new oil-flow cell emerges above the interface near the axis. This cell disappears as the interface approaches the lid. The water separates from the sidewall, reaches the lid, and forms a column. As the rotation is decreased, the scenario reverses, but the flow states differ from those for the increasing rotation, i.e., a hysteresis is observed. The numerical simulations agree with the experiment and help explain the flow metamorphoses.

1. Introduction

Swirling two-fluid flows attract the attention of researchers due to applications in aerial vortex bioreactors and are of fundamental interest due to striking features including their nontrivial topology [1-5]. Fujimoto & Takeda [4] experimentally studied interface patterns of a flow of water and silicone oil driven by the rotating lid in a vertical sealed cylindrical container. As the rotation intensifies, the interface becomes strongly and unusually deformed. The experiment of Tsai et al. [5] revealed vortex breakdown in the oil flow, and the numerical simulations by Carrion et al. [3] predicted that vortex breakdown also occurs in the water flow.

The current experimental and numerical study addresses a similar flow of water and sunflower oil in a sealed vertical cylindrical container driven by the lid rotating with angular velocity ω. As ω increases, the oil-water interface deforms upward near the axis and downward near the sidewall as typical of water spouts. At $\omega = \omega_1$, the flow separates from the sidewall. At $\omega = \omega_{up}$, the interface touches the rotating lid and water spreads over the near-axis lid part. A bell-shape water column forms near the axis, separated from the sidewall and extended from the bottom to the lid. The resulting density stratification with water (oil) being located near the axis (at the periphery) is unstable for fast rotation. Accordingly as ω further increases, the interface breaks and water mixes with oil. When ω is decreases before the interface breaks, the water separates from the lid at $\omega = \omega_{down}$, which is slightly smaller than ω_{up}, and touches the sidewall at $\omega = \omega_2 < \omega_1$.

Our numerical and experimental results agree for the dependence of the water height at the axis on the rotation strength. The numerical study allows for detailed investigations of topological metamorphoses occurring in this flow. As the rotation intensifies, first the water flow becomes two-cellular, and then a new cell emerges and disappears in the oil flow. Thin circulation water layer adjacent to the interface emerges at a weak rotation when the interface is almost horizontal, has the bubble-ring shape in some ranges of ω, and still exists as the interface becomes nearly vertical.

2. Experimental setup and numerical technique

Figure 1(a) is a schematic of the experimental setup, showing the cylindrical container (1), CCD camera (2), stepping motor (3), LED 250W lamp (4) and reflecting white screen (5) [6,7]. The apparatus was housed in a darkened room, with lighting, provided by a LED 250W lamp reflected off a white sheet of paper. The photos of interface were shot by CCD 6-megapixel camera CASIO EX-F1. The cylindrical container is made of transparent optical glass with an inner radius of 45.75 mm and a height of 126 mm. The lid of radius R = 45 mm can be positioned at a varying height. The container is filled with tap water ($0 < z < h_w$, dark in figure 1) and sunflower oil ($h_w < z < h$, light in figure 1); z is the distance from the container bottom. Here we use h = R and $h_w = 0.2R$; these values are relevant for studying the hysteresis and the column formation in this flow.

At the room temperature of 22.6˚C, the fluid densities and kinematic viscosities are ρ_w = 1000 kg/m^3, ρ_o = 920 kg/m^3, ν_w = 1 cSt, and ν_o = 55 cSt. Hereafter subscripts "w" and "o" denote "water" and "oil". The oil-water interface tension is σ_{ow} = 26 mN/m. The container is still except for the lid, which can rotate with angular velocity ω driven by the stepping motor. The rotation strength is characterized by the Reynolds number $Re = \omega R^2/\nu_o$; Re = 100 corresponds to approximately 0.5 RPS. For the Re range considered here, the variation in ω during a revolution is less than 0.3%.

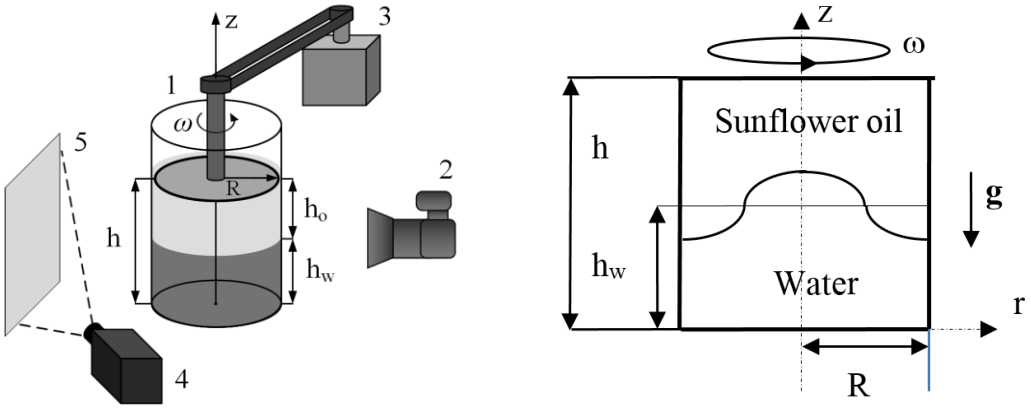

(a) (b)

Figure 1. Schematic of experimental set up (a) and the numerical problem (b).

Figure 1(b) is a schematic of the numerical problem. One control parameter is aspect ratio, H = h/R. Another control parameter is the dimensionless water height, $H_w = h_w/R$. These values are fixed here: H = 1 and H_w = 0.2 to be consistent with the experiment. For the numerical procedure, it is convenient to introduce the Reynolds number based on the water viscosity, $Re = \omega R^2/\nu_w$.

To simulate the nonlinear problem for the basic flow, we use a numerical technique which is a variation of that described in detail by Herrada & Montanero [8]. First, the heavy-fluid (water) and light-fluid (oil) regions are mapped onto the standard square domain. Then, each variable (velocities, pressure and the interface shape) and all its spatial and temporal derivatives, which appear in the transformed equations, are composed as a single symbolic vector. The next step is to use a symbolic toolbox to calculate the analytical Jacobians of all the equations with respect to all the symbolic

vectors. Using these analytical Jacobians we generate functions which then are evaluated point by point in the square domains. Then, we carry out the spatial and temporal discretization of the problem. To summarize, the numeric procedure includes the mapping of water and oil regions, the proper spatial and temporal discretization creating the discrete Jacobian matrix of the Newton procedure. For the established flow, we get the final steady solution through an unsteady process. The final step is to set up the numerical matrices allowing us to solve the problem by using a Newton procedure for the basic steady flow and by solving the generalized eigenvalue problem for disturbances [1-3].

3. Topological metamorphoses of flows

It is instructive to start with a creeping flow and to gradually increase the Reynolds number. Figure 2 depicts streamlines at Re_o = 1 (a), 100 (b) and 300 (c). The rotating lid pushes the upper fluid to periphery near the lid, as the upper arrow indicates in figure 2(a), and thus drives the clockwise circulation in CRO1; CR is an abbreviation for circulation region and O denotes the oil.

Near the interface, the oil moves toward the container axis, r = 0, and tends to drive the anticlockwise circulation of water. On the other hand, the oil flow transports the angular momentum from the lid to the interface. This angular momentum rotates the water. The centrifugal force pushes the water toward the sidewall near the interface and tends to drive the clockwise circulation of water.

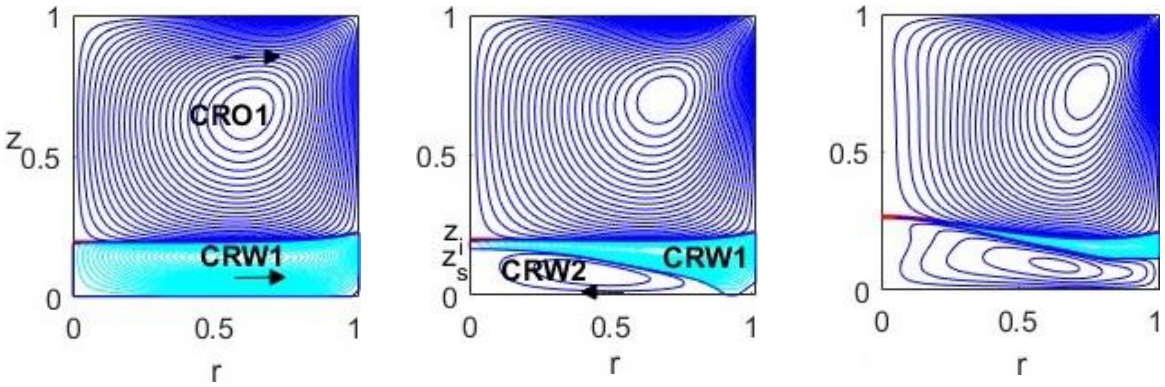

(a) (b) (c)

Figure 2. Clockwise circulation emerges in water as Re increases: Re_o = 1 (a), 100 (b) and 300 (c).

Thus, the two factors, (*i*) swirl and (*ii*) meridional velocities at the interface, push the water in opposite directions. At Re_o = 1, the swirl velocity at the interface is smaller than ωR by three orders of magnitude [3]. This yields that factor (*ii*) dominates over (*i*) and drives the bulk anticlockwise circulation, marked as CRW1 in figure 2(a), where W denotes the water.

In figure 2(a), the water moves upward in the bulk flow near the sidewall and thus blocks the downward transfer of the angular momentum from the interface. The angular momentum is transported toward the axis along the interface and then downward near the axis in the water domain. Therefore, the swirl effect is the strongest near the axis-bottom intersection where a cell of clockwise circulation emerges as Re_o increases, and factor (*i*) strengthens; this cell is denoted as CRW2 in figure 2(b). CRW1 separates from the bottom and becomes thin in figure 2(c).

Figure 3 shows photos of the oil-water interface (left) and streamline pattern (right) as Re increases. Figure 3(a) illustrate the development of the interface hump shape. At Re_o = 687 (figure 3(b)), the water separates from the sidewall. At Re_o = 840, the interface has the "bell" shape with its top being close to the lid as figure 3(c) illustrates. At Re_o = 865, the rising interface reaches the rotating lid. Then, the water spreads over a near-axis area of the lid as figure 3(d) shows at Re_o = 935. The centrifugal force pushes water, located near the lid, away from the axis, thus increasing the water radius at the lid and developing a "neck" in the interface upper part.

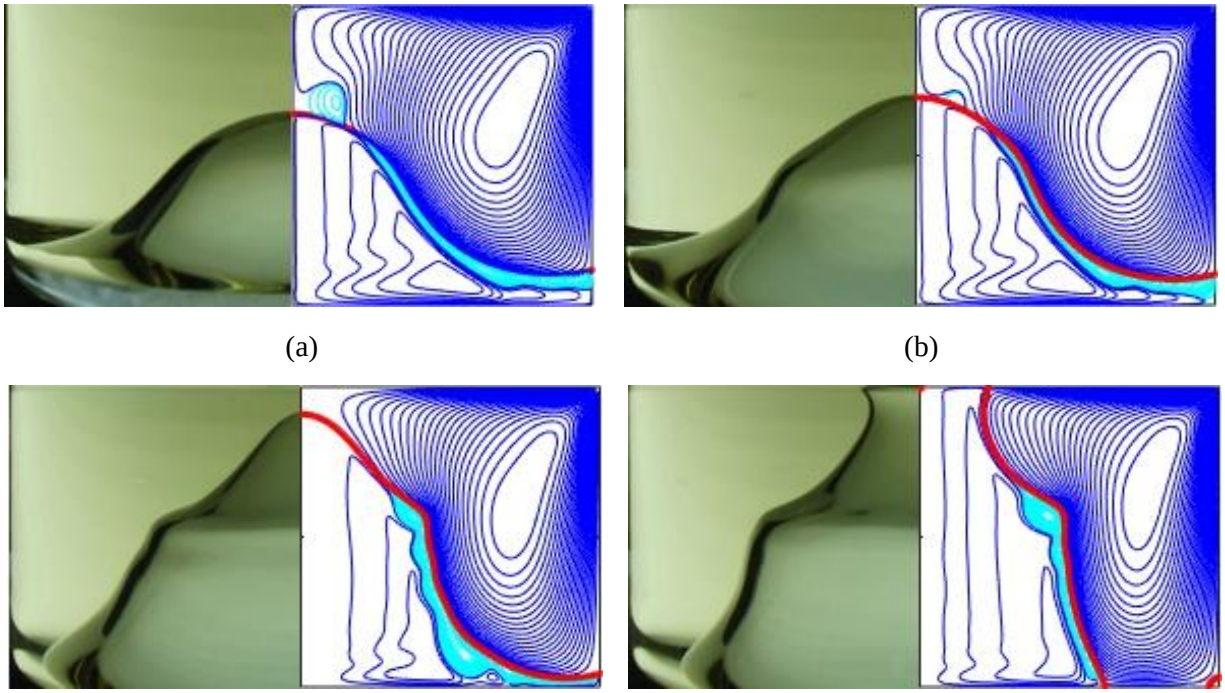

Figure 3. Interface shapes (left) and streamline pattern (right) at Re_o=650 (a), 687 (b), 840 (c), 935 (d).

Figure 4 characterizes the hysteresis by presenting the dependence of the interface height at the axis, h_i, on the rotation speed, Re. To measure the interface height at the axis, we use the experimental technique described in detail by Naumov et al [6, 7]. The interface height at the axis was measured by a laser beam and a precise scale. A semiconductor laser was fixed on the coordinate device. The laser beam was shifted up starting from the bottom along z-axis with a step of 0.1 mm until the reflection of laser beam from the interface terminates and the beam becomes tangent to the interface, touching the interface top.

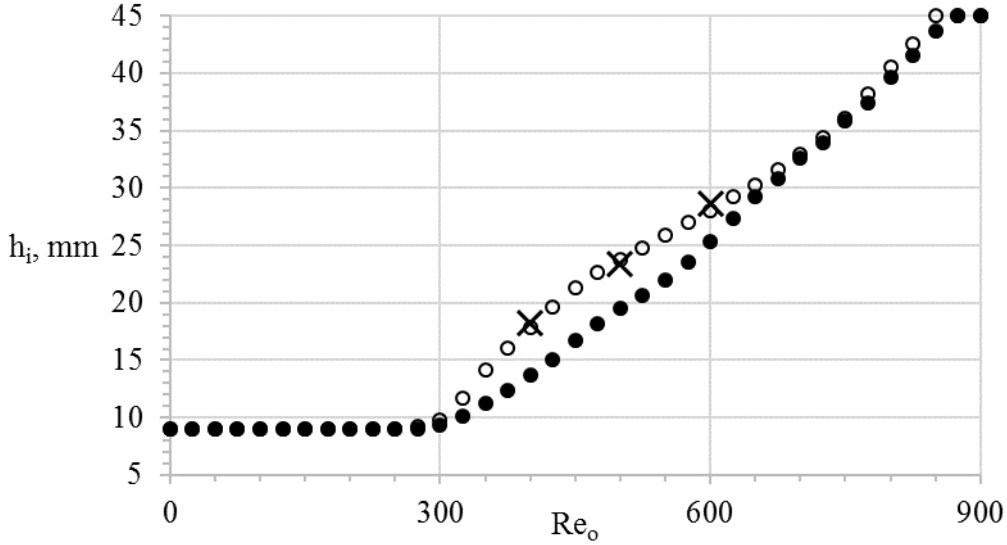

Figure 4. Dependence of interface height on the rotation speed as Re_o increases (filled circles) and decreases (experimental (empty circles) and numerical (crosses) results).

First, Re_o was increased from 0 with an increment ≤ 25. The results are presented by filled circles in figure 4. The interface height looks unchanged up to Re_o, being around 300, and then linearly grows with Re_o. The slope slightly increases for Re_o > 687. It seems that this occurs due the interface becomes separation from the sidewall. The horizontal line is for the interface attached to the lid for $Re_o > Re_{ol1} = 865$. Next, Re_o was decreases with the step down being ≤ 25. The results are presented by empty circles in figure 4. Interpolation estimates that the interface separates from the lid at $Re_o = Re_{ol2} = 854$. While the difference, $Re_{ol1}–Re_{ol2}$, is small and close to the measurement accuracy, the difference of the interface height at the axis, Δh_i, for the filled and empty circles remarkably increases for Re_o < 650 (figure 5). This increase is due to the fact that the interface is detached from the sidewall for the emplty circles while it is attached to the sidewall for the filled circles. The difference diminishes as the interface touches the sidewall at $Re_o = 343$ for decreasing Re_o (figure 5).

Figure 4 also shows the numerical (crosses) results describing the dependence of the interface height at the axis on decreasing Re_o. The numerical results correspond to Re_o = 600, 500, and 400 where the water is separated from the sidewall. Since our software is not applicable for such flow patterns (because of the applied mapping), these simulations were performed with the help of the commercial software FLUENT. The interface-sidewall contact angle is taken as 120° at Re_o = 600, 100° at Re_o = 500, and 80° at Re_o = 400.

It is known [9], that the contact angle is a monotonically increasing function of the interface velocity at a wall, U, and has a jump at U = 0. Therefore, the angle depends on the flow prehistory even for the established steady state. The jump value depends among others on the wall-material features such as roughness and wetting. Since it is problematic to experimentally determine this dependence, here the angle is chosen to better fit the experimental data.

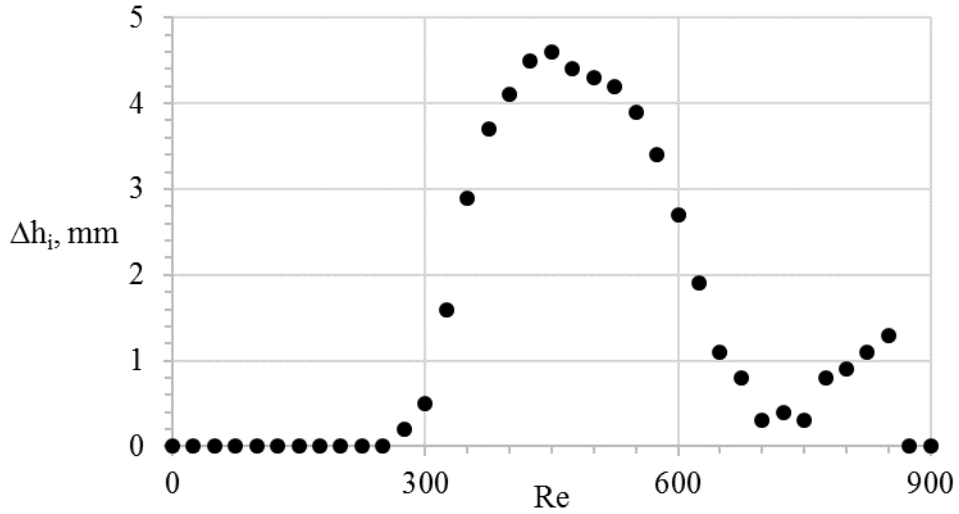

Figure 5. Dependence of the interface height difference at the axis on Re_o.

The flow states differ for increasing and decreasing Re_o, that is well observed in figure 6 at Re_o = 450 where Δh_i have maximal value of 4.6 mm. Figure 6(a) corresponds to increasing Re_o, and figure 6(b) corresponds to decreasing Re_o. The water is well attached to the sidewall in figure 6(a) while the water is still detached from the sidewall in figure 6(b). Accordingly, the water height at the axis is significantly smaller in figure 6(a) than that in figure 6(b). As Re_o further decreases, the water attaches the sidewall at Re_o = 343.

To sum up, the experimental observations reveal a hysteresis related to the interface separation from and reattachment to the sidewall with the hysteresis range being $343<Re_o<687$.

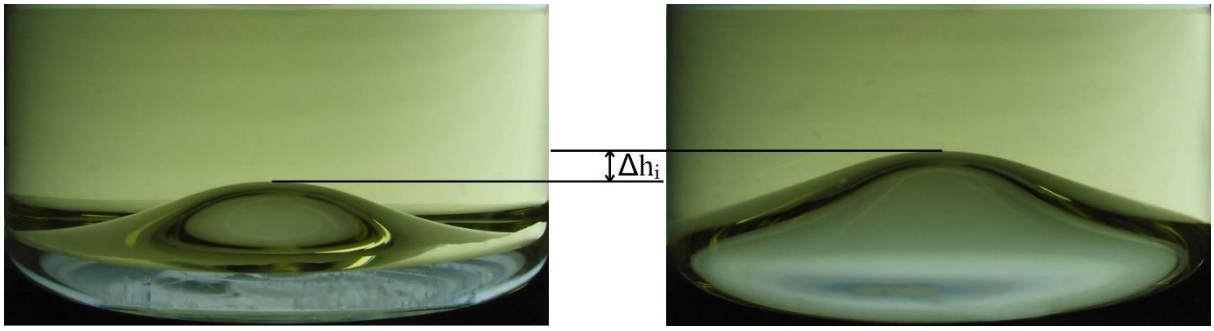

(a) (b)

Figure 6. Two different flow states at Re_o =450 (a) as Re_o increases and (b) as Re_o decreases, where the difference of the interface height have maximal value 4.6 mm.

4. Conclusion

This pater explores two intriguing fluid-mechanics phenomena: (a) the formation of water column and (b) hysteresis in a water-spout flow. To observe large interface deformations in a laboratory, we study a water-sunflower-oil flow. The close densities and very different viscosities of water and oil allow analyzing the phenomena in a compact set-up: a cylindrical container of 45 mm in both radius and height, filled with 20% (80%) volume fraction of water (oil). The rotating lid of container drives the meridional circulation and swirl of both liquids.

The numerical calculations and the visual experimental observations have revealed that as the rotation speeds up, the interface rises near the axis, descends near the sidewall, separates from the sidewall, touches the lid, and then destroys. As rotation decreases, the interface pattern differs from that as the rotation increases. The hysteresis is quantitatively explored by measuring the dependence of the interface height at the axis, h_i, on the rotation strength, Re_o. The numerical and experimental results agree concerning the interface shape and height at the axis.

To investigate flow features (especially topology) in more detail, the numerical simulations were performed with the help of the original software [8]. The simulations have revealed that as Re_o increases, the water flow becomes two-cellular, ascending (descending) along the axis near the bottom (interface). The ascending circulation expands and touches the interface while the opposite water circulation shrinks into a thin layer adjacent to the interface. A new cell appears and disappears in the oil flow. The agreement of the numerical and experimental results verifies the paper findings.

5. Acknowledgments

Research was supported by the Russian Science Foundation (Project № 14-29-00093).

References

[1] Balci A, Brøns M, Herrada M A and Shtern V N 2015 *Fluid Dyn. Res.* **47** 065503
[2] Herrada M A and Shtern V N 2014 *J. Fluid Mech*. **744** 65-88
[3] Carrión L, Herrada M A and Shtern V N 2017 *Phys. Fluids* **27** 032109
[4] Fujimoto S and Takeda Ya 2009 *Phys. Rev.* E **80** 015304(R)
[5] Tsai J C, Tao C Y, Sun Y C, Lai C Y, Huang K H, Juan W T and Huang J R 2015 *Phys. Rev.* E **92** 031002(R)
[6] Naumov I V, Sharifullin B R and Shtern V N 2017 *J. Eng. Thermophys.* **26** 391-8
[7] Naumov I V, Sharifullin B R and Shtern V N 2017 *J. Phys. Conf. Ser.* **899** 032015
[8] Herrada M A and Montanero J M 2016 *J. of Comput. Phys.* **306** 137-47
[9] Eral H B, 't Mannetje D J C M and Oh J M 2013 *Colloid & Polymer Sci.* **291** 247-60